DIRECT NUMERICAL SIMULATION OF THE TURBULENT MOMENTUM AND HEAT TRANSFER IN AN INTERNALLY HEATED FLUID LAYER

G. Grötzbach

Kernforschungszentrum Karlsruhe, Institut für Reaktorentwicklung
Postfach 3640, 7500 Karlsruhe, Fed. Rep. of Germany

ABSTRACT

The natural convection in an infinite horizontal fluid layer with internal heat generation and a Prandtl number Pr=6 is investigated using the direct numerical simulation method. The results are in good agreement with experimental data. For moderate Rayleigh numbers counter-gradient heat fluxes have been found in the core of the flow. The predicted statistical data of turbulence show that first order models like the eddy conductivity and -ε models cannot account for this phenomenon. Some additional results, especially for terms containing pressure fluctuations, are discussed for use in the calibration of second order statistical models which would be more appropriate to this flow than first order models.

1. INTRODUCTION

The natural convection in horizontal fluid layers with internal heat generation is of interest as a model for certain environmental, geophysical, astrophysical and nuclear engineering heat transfer problems. For the description of turbulent heat transfer within such layers direct numerical simulation and statistical turbulence models are used. In the direct methods the complete, three-dimensional, non-steady conservation equations are applied. No model assumptions are needed but a very fine spatial discretization is necessary to resolve the smallest scales of turbulence. This method has been applied previously for low and high Rayleigh numbers in two dimensions [1,2,3] and for moderate Rayleigh numbers in three dimensions [4]. The statistical methods are based on time averaged equations. Models must be introduced to represent the total information about turbulence. The applied statistical models are "first order models" like the eddy conductivity concept [5,6,7] and the k-ε-model [8]. From experiments as in [9] heat transfer data across the boundaries and a few temperature profiles have been obtained, from which some turbulent heat fluxprofiles have been estimated in [10]. This information is not sufficient to determine the coefficients for higher order statistical turbulence models for this type of flow. This in particular holds with respect to terms which involve pressure fluctuations.

In this paper turbulence data are investigated which are obtained from direct numerical simulations. The three-dimensional and time-dependent model in the computer code TURBIT-3 [11] is used to cover a cubic domain between an infinite upper and lower horizontal wall at equal temperature. The spatial grids with up to $64^2 \cdot 32$ nodes have sufficient spatial resolution to resolve all relevant scales of turbulence at Rayleigh numbers up to 110 times the critical value at a Prandtl number of six [4]. The model contains no tuning parameters. Hence the predicted turbulence data can be used to calibrate statistical turbulence models like those used in [5,7,8,12].

2. NUMERICAL SIMULATION MODEL

The model TURBIT-3 [11,13] is based on the complete, three-dimensional, non-stationary conservation equations for mass, momentum and heat. The validity of the Boussinesq approximation is assumed. Cartesian coordinates are used with x_1 and x_2 horizontal and x_3 directed upwards.

A finite difference scheme of these equations is deduced by integrating formally over a mesh cell volume $V = \Delta x_1 \Delta x_2 \Delta x_3$. Application of the Gaussian theorem to the volume average of partial derivatives directly gives a finite difference form $\delta_i {}^i\bar{u}_i$ for surface average values ${}^i\bar{u}$, where u_i is a velocity component and i indicates the direction normal to the mesh cell surface [14]. Averaging of the convective terms gives unknown terms which represent the momentum and heat fluxes of those vortices not resolved by the grid. These subgrid scale terms are neglected here. A staggered grid is used with the velocities defined on mesh cell surfaces, and with the volume averages of pressure, $\overline{p}$, and temperature, $\overline{T}$, defined in the mesh cell centers. An explicit Euler-leap frog scheme is applied for time integration.

In both horizontal directions periodicity is assumed with periodicity lengths $X_1 = X_2 = 2.8 \cdot D$, D = channel height. In the vertical direction the velocities are set to zero at the walls, and the wall shear stresses and wall heat fluxes are approximated by linear finite difference approximations. The prescribed wall temperatures T_{wi} are held equal and constant in space and time.

The node numbers N_i of the grids chosen for our simulations are specified in table 1. For a Prandtl number of six we consider one case with a subcritical Rayleigh number of $Ra = g\gamma\dot{Q}D^5/(\nu a\lambda) = 3 \cdot 10^4$, where $\dot{Q}$ = volumetric heat source, one from the laminar to turbulent transition range, and one

for turbulent flow. The grids of all three cases satisfy the spatial resolution requirements specified in [4] to justify the neglection of the subgrid scale terms and to choose linear wall approximations.

Table 1: Case specifications and time intervals.

Ra	Da_o	N_1	N_2	N_3	t_{max}	Nt	CPU-time hours/IBM	Nt_{av}
$3 \cdot 10^4$	8.0	16	8	16	12.0	2400	0.61/168	21
$3.5 \cdot 10^5$	10.26	16	16	16	75.6	5760	2.96/168	26
$4 \cdot 10^6$	15.72	64	64	32	40.2	4040	38.2/3033	15

To get a universal presentation of the results the basic equations are normalized with the length D, the time D/u_o, the velocity $u_o = (g\gamma\Delta T_o D)^{1/2}$, and the temperature $\Delta T_o = <T_{max} - T_w>$. The latter is calculated using the dependence between the Damköhler and Nusselt numbers at the lower, Nu_1, and upper wall, Nu_2: $Da_o = QD^2/(\lambda\Delta T_o) = Nu_1 + Nu_2$. The Da_o-values given in table 1 have been preestimated from the correlations of [15].

3. VERIFICATION OF THE NUMERICAL RESULTS

Starting from quasi-random initial conditions specified in [4] the finite difference equations are integrated in time until steady state conditions, in a statistical sense, are established for a period suitable for evaluation. The respective problem times t_{max}, number of time steps Nt, and computer times needed are also indicated in table 1. To obtain reasonable statistical data from the time dependent numerical results, averages <y> are formed for a calculated variable y over horizontal planes and over Nt_{av} Euler time steps.

The temperature profiles calculated in such a manner are compared to experimental data [9] in figure 1. For the subcritical Rayleigh number the initially disturbed flow goes to rest and causes a conduction controlled temperature profile. The supercritical cases show increasing temperature gradients near the walls for increasing Rayleigh numbers. The larger gradients near the upper walls at $x_3 = 1.0$ indicate that most thermal energy released in the channel is transferred upwards. Nevertheless, the maximum temperature also moves nearer to the upper wall. Thus, we have to expect counter-gradient heat fluxes in the inner part of the channel.

The calculated temperature profiles agree with the experimental data except for the results for the highest Rayleigh number at $0.3 < x_3 < 0.8$. In that region an increase in temperature is predicted by TURBIT-3, but a nearly isothermal core is found in the experiment. In [4] contour line plots of instantaneous temperature fields from the same simulation are compared to interference pictures from [16]. The agreement found there confirms the calculated mean temperature profile. Further, those figures show that the temperature increase in the center of the channel is forced by the rapid penetration of narrow cold plumes released from the upper wall. The plumes decelerate and expand below the center of the channel. There, finally the plumes come into thermal equilibrium with the ambient fluid.

Further experimental data on flow structures

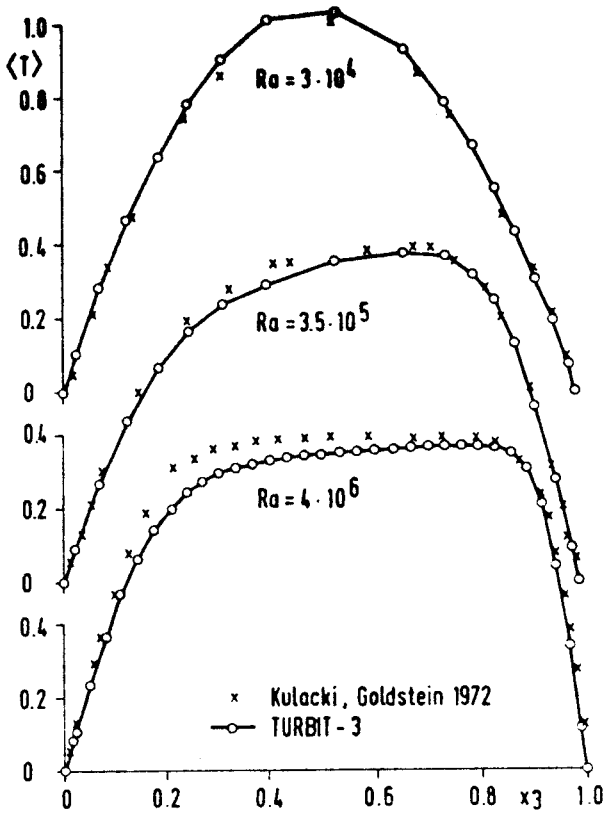

Fig. 1: Vertical time mean temperature profiles.

observed in horizontal planes and on the Nusselt number confirm the numerical results [4].

4. PREDICTED TURBULENCE DATA

Having verified the numerical results we now can use these simulation results to calculate turbulence quantities. Such data have not yet been determined by experiments for this type of flow.

4.1. The eddy conductivities

For a stationary turbulent flow in a channel with infinite horizontal extensions the Reynolds-time-averaging procedure reduces the set of conservation equations to the one-dimensional thermal energy equation. Models must be introduced for the unknown vertical turbulent heat flux $<u_3'T'>$, where' denotes the deviation from the local time mean value. The simplest approach is to assume gradient diffusion proportional to a local eddy conductivity $\varepsilon_H = -<u_3'T'>/(\partial<T>/\partial x_3)$. Such a model has been used in [5]. For a channel with an adiabatic lower wall a model has been proposed in [7]. From experiments profiles for $/\varepsilon_H/$ have been evaluated from measured temperature profiles [10].

The eddy conductivities given in figure 2 have been determined from the calculated turbulent heat flux, $<\overline{^3u_3'}\,\overline{^v T'}>$, given in [4], and the calculated local temperature gradient, $\delta_3 <\overline{^v T}>$. The predicted ε_{Hi} are positive near the lower wall, i = 1, and the upper wall, i = 2, but they are, as expected,

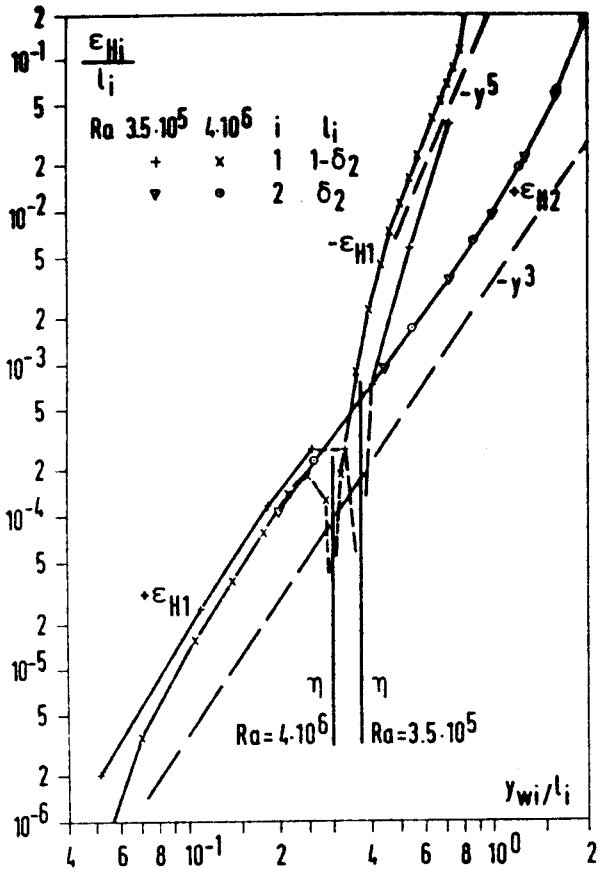

Fig. 2: Calculated eddy conductivity profiles. y_{wi} is the distance to the wall i; l_i is the local length scale; $\eta = Nu_1/(Nu_1 + Nu_2)$.

negative in the range $\eta < x_3 < x_3(T_{max})$, that means between the plane of zero turbulent heat flux and of maximum temperature. The profiles for both Rayleigh numbers for the upper wall coincide on a single line having a slope of about three. This is forced by the normalization used in this paper at which the length scale D has been replaced by the thermal boundary layer thickness $\delta_2 = 1/Nu_2$, with Nu_2 (Ra = $3.5 \cdot 10^5$) = 7.28 and Nu_2 (Ra = $4 \cdot 10^6$) = 12.85. This length scale is representative for the thickness of the unstable upper layer. The lower part of the profile follows approximately the same line, but the coincidence is poorer because the length scale $1-\delta_2$ chosen there does not account for the differences in η. The same restriction holds also for the negative part of the profile where we find an even steeper, but not so marked slope.

4.2. Terms of the energy-length-scale approach

This approach has been applied to the internally heated convection problem in form of the k-ε model [8]. There, the eddy conductivity is replaced by $\varepsilon_H \sim k^2/(\varepsilon Pr_t)$, where Pr_t is the turbulent Prandtl number, $k \equiv E$ is the kinetic energy, and ε is its dissipation. E and ε are calculated from additional model equations. Appropriate data are missing to calibrate the coefficients for natural convection problems.

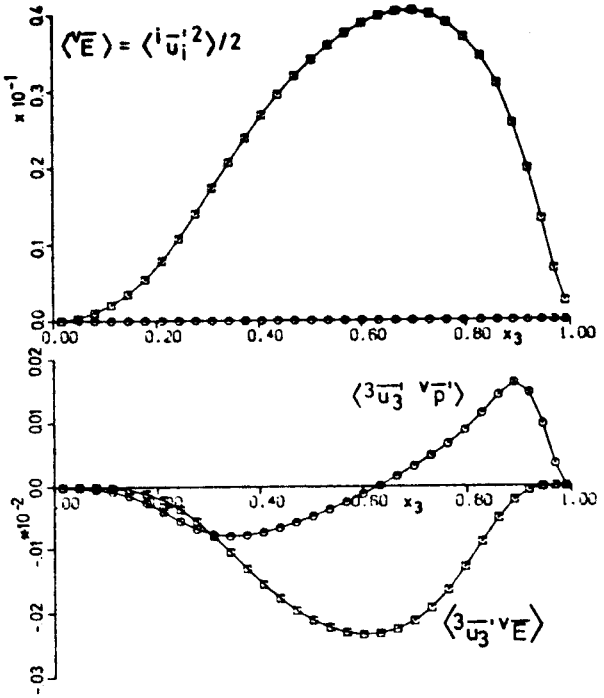

Fig. 3: The kinetic turbulence energy and the closure terms for the kinetic energy equation; Ra = $4 \cdot 10^6$.

In figure 3 numerical results are given for the kinetic energy and for terms of the respective conservation equation. The energy is very small in the stable region near the lower wall. Its maximum is outside the unstable upper wall layer below the temperature maximum (fig. 1), and also below the maximum of the production term which is at $x_3 \approx 0.8$ [4]. The reason is found from the two crosscorrelations contained in fig. 3, which represent the unkonwn closure terms in the turbulent diffusion term, $-\delta_3 \langle {}^{3}\overline{u_3'}\,{}^{v}\overline{E} \rangle - \delta_3 \langle {}^{3}\overline{u_3'}\,{}^{v}\overline{p'} \rangle$. The increase of both correlations for $0.8 < x_3 < 0.9$ signifies a strong negative diffusion which extracts energy. The energy is transported to the lower stable half of the channel where the turbulent diffusion can be deduced to be positive. The gradients of both crosscorrelations are comparable in size except near the walls where the pressure diffusion term predominates. Profiles for the total diffusion, production, and dissipation terms are discussed in [4].

To circumvent the problem of formulating a vertical profile for Pr_t an extended k-ε-model can be used. The alternative given in [17] is $\varepsilon_H = C_H\, E\, E_T/\varepsilon_T$, where C_H is an additional unknown coefficient, $E_T = \langle T'^2 \rangle /2$ is the "energy" of temperature fluctuations, and ε_T is the dissipation of E_T.

The calculated temperature-rms-values, $\sqrt{\langle {}^{v}T'^{2} \rangle} = \sqrt{2\,E_T}$, and terms of the conservation equation for E_T are given in figure 4. The temperature fluctuations are considerably greater than zero in the lower stable layer. The maximum is found in the unstable layer slightly above the position of the temperature maximum (fig. 1). The crosscorrelation, $\langle {}^{3}\overline{u_3'}\,{}^{v}\overline{E_T} \rangle$, which is the unknown term in the equation for E_T, looks like $\langle {}^{3}\overline{u_3'}\,{}^{v}\overline{E} \rangle$ in fig. 3, or like

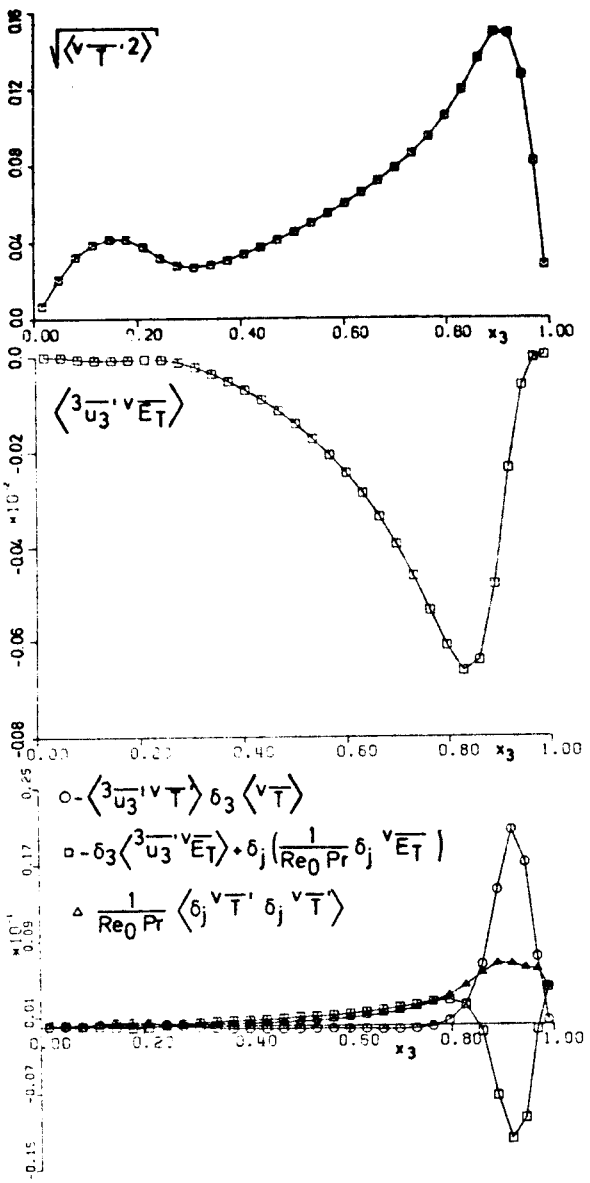

Fig. 4: The temperature rms-value, the closure term and the terms of production, diffusion, and dissipation in the equation for E_T; $Re_0 = u_0 D/\nu$; $Ra = 4 \cdot 10^6$.

the negative turbulent heat flux except for the missing pronounced change in sign in the lower wall layer and the thicker upper boundary layer. The total diffusion of E_T is also given in figure 4 together with the production and dissipation terms. The negative diffusion near the upper and the lower wall compensates the difference between production and dissipation in this range. The extracted "energy" of temperature fluctuations is transfered to the center of the channel where a small negative production needs to be compensated. Qualitatively, the behaviour found for the upper part of the channel is comparable to that of terms of the kinetic energy equation in the total vertical extension.

The calculated profile of the coefficient C_H is

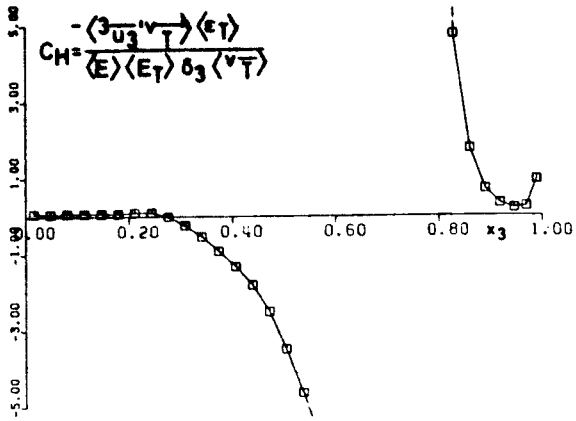

Fig. 5: Coefficient of the k-ε-heat flux model; $Ra = 4 \cdot 10^6$.

given in figure 5. Constant values are found near the lower wall where molecular conduction predominates. Negative values are predicted in the middle of the channel, and a strongly space-dependent profile is calculated for the most sensitive upper wall layer where most heat is transfered by convection.

4.3. Terms of the second-order-moment approach

The most appropriate way to account for counter-gradient heat fluxes would be to use models for the conservation equation of $\langle u_3' T'\rangle$. The model applied by Daly [12] to Bénard convection in an infinite channel is an example for this concept. The turbulent heat flux is calculated via a turbulent Prandtl number from an equation for the time-dependent mean value of the turbulent shear stress.

The problematic terms in the equations for $\langle u_i' u_j'\rangle$ are the pressure strain terms shown in figure 6. The kinetic energy is non-equally distributed between the three velocity components. In the core most energy is associated with the vertical velocity fluctuations u_3' (compare also to figure 3). Nevertheless, the pressure-strain terms, which are also called the tendency-toward-isotropy terms, show only minor energy transfer from the vertical (i=j=3) to the horizontal velocity fluctuations (i=j=1,2). This indicates an only weak interaction between the downflowing plumes and the ambient fluid. Near the upper wall less energy is associated with the vertical velocity fluctuations although this component is the only one excited directly by the buoyancy term. This predominance of the horizontal velocity fluctuations is caused by the pressure-strain terms which transfer most energy in the wall region from the vertical to the horizontal velocity components.

The pressure terms contained in the equation for the turbulent heat flux $\langle u_3' T'\rangle$ are given in figure 7. It can be deduced that the pressure diffusion term $-\delta_3\langle {}^{v}\overline{p}'\,{}^{v}\overline{T}'\rangle$ strongly reduces the turbulent heat flux for $x_3 > 0.9$, and increases it near $x_3 \approx 0.8$ where we find the maximum of the turbulent heat flux. The pressure-scrambling term $\langle {}^{v}\overline{p}'\delta_3\,{}^{v}\overline{T}'\rangle$ is negative all over the channel. It mainly reduces the correlations between u_3' and T' near the upper wall too.

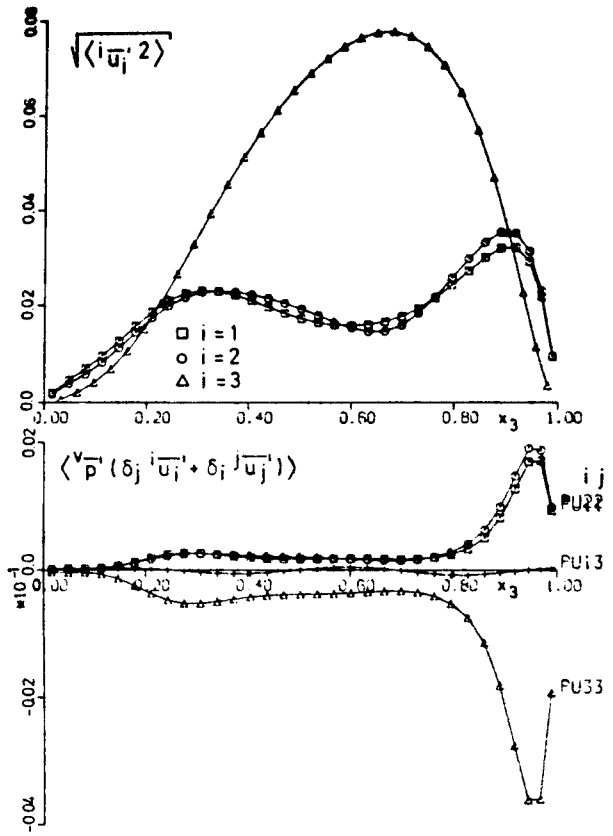

Fig. 6: The transfer of kinetic energy by the pressure-strain terms; Ra = $4 \cdot 10^6$.

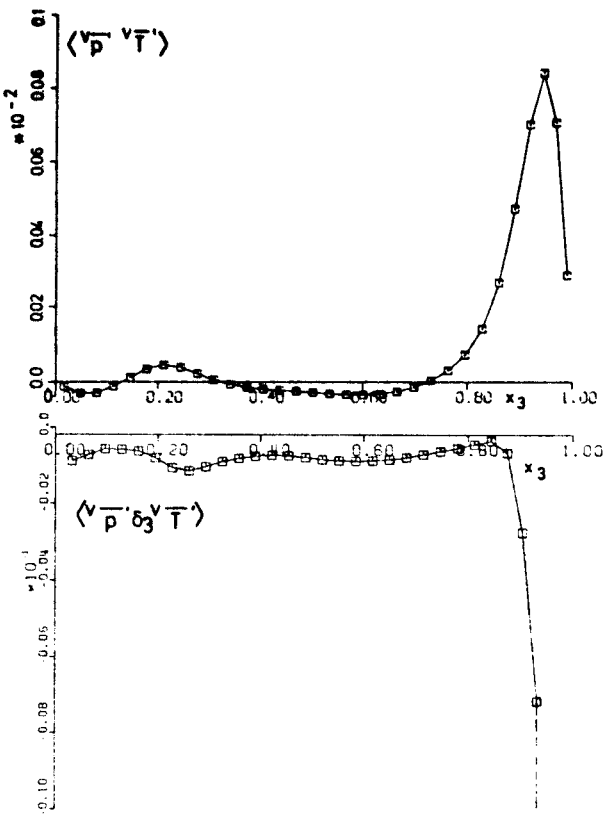

Fig. 7: The pressure-temperature correlation and the pressure-scrambling term; Ra = $4 \cdot 10^6$.

5. CONCLUSIONS

For moderate Rayleigh numbers of Ra $\leq 4 \cdot 10^6$ counter-gradient heat fluxes have been found in a substantial part of the turbulent core of the flow. In this region the eddy conductivities predicted by the direct numerical simulation model are correspondingly negative. Thus, the eddy conductivity concept is no proper tool to model the turbulent heat flux in the parameter range under consideration. Scales have been found for the eddy conductivities which allow to correlate at least the profiles near the upper wall and, with somewhat less accuracy, also near the lower wall. Two versions of the k-ε model have been considered. Both suffer from the same problem as the eddy conductivity concept because gradient diffusion is assumed too. For larger Rayleigh numbers this problem will persist because the turbulent core becomes virtually isothermal in a larger domain. To circumvent this problem one should use second order models based on turbulent shear stress and heat flux equations. For this approach several correlations containing turbulent pressure fluctuations have been predicted. It seems that these important terms have not been determined experimentally. Thus, the present numerical predictions give the required basis for the development of statistical turbulence models for this type of flow.

6. ACKNOWLEDGEMENTS

The author kindly appreciates the discussions with Dr. U. Schumann and the comments by Dr. Ch. Homann, both from the Institut für Reaktorentwicklung, Kernforschungszentrum Karlsruhe.

7. REFERENCES

1. Peckover, R.S., Hutchinson, I.H., Convective rolls driven by internal heat sources, Physics of Fluids, vol. 17, pp. 1369-1371, 1974.
2. Reineke, H.H., Numerische Berechnung der thermohydraulischen Vorgänge in einer Kernschmelze, Diss., Techn. Universität Hannover, 1974.
3. Emara, A.A., Kulacki, F.A., A numerical investigation of thermal convection in a heat-generating fluid layer, J. Heat Transfer, vol. 102, pp. 531-537, 1980.
4. Grötzbach, G., Spatial resolution requirements for numerical simulation of internally heated fluid layers, in Numerical Methods in Laminar and Turbulent Flow, ed. C. Taylor, B.A. Schrefler, pp. 593-604, Pineridge Press, Swansea, 1981.
5. Mayinger, F., Jahn, M., Reineke, H.H., Steinberner, U., Untersuchung thermohydraulischer Vorgänge sowie Wärmeaustausch in der Kernschmelze, Abschlußbericht BMFT-RS 48/1, Teil I, 1975.

6. Biasi, L., Castellano, L., Holtbecker, H., Molten pool theoretical studies, PAHR-Information Exchange, ANL 78-10, Argonne, November 2-4, 1977.
7. Cheung, F.B., Natural convection in a volumetrically heated fluid layer at high Rayleigh numbers, Int. J. Heat Mass Transfer, vol. 20, pp. 499-506, 1977.
8. Steinberner, U., Reineke, H.H., Turbulent buoyancy convection heat transfer with internal heat sources, Proc. 6th Int. Heat Transfer Conf., Toronto, vol. 2, pp. 305-310, 1978
9. Kulacki, F.A., Goldstein, R.J., Thermal convection in a horizontal fluid layer with uniform volumetric energy sources, J. Fluid Mech., vol. 55, pp. 271-287, 1972.
10. Kulacki, F.A., Goldstein, R.J., Eddy heat transport in thermal convection with volumetric energy sources, Proc. Fifth Int. Heat Transfer Conf., Tokyo, vol. 3, pp. 64-68, 1974.
11. Grötzbach, G., Numerical investigation of radial mixing capabilities in strongly buoyancy-influenced vertical, turbulent channel flows, Nuclear Engineering and Design, vol. 54, pp. 49-66, 1979
12. Daly, B.J., A numerical study of turbulence transitions in convective flow, J. Fluid Mech., vol. 64, pp. 129-165, 1974.
13. Grötzbach, G., Direct numerical simulation of laminar and turbulent Bénard convection, J. Fluid Mech., to appear.
14. Schumann, U., Subgrid scale model for finite difference simulations of turbulent flows in plane channels and annuli, J. Comp. Phys., vol. 18, pp. 376-404, 1975
15. Baker Jr., L., Faw, R.E., Kulacki, F.A., Post-accident heat removal I: Heat transfer within an internally heated nonboiling liquid layer, Nucl. Science Engng., vol. 61, pp. 222-230, 1976.
16. Jahn, M., Holographische Untersuchung der freien Konvektion in einer Kernschmelze, Diss., Techn. Universität Hannover, 1975.
17. Meroney, R.N., An algebraic stress model for stratified turbulent shear flows, Comp. Fluids, vol. 4, pp. 93-107, 1976.

Heat Transfer 1982

Proceedings of The Seventh International Heat Transfer Conference

München, Fed. Rep. of Germany

Edited by
U. Grigull, E. Hahne, K. Stephan,
and J. Straub

in cooperation with the members of the
International Scientific Committee

A. E. Bergles, M. Cumo, N. Epstein,
R. J. Goldstein, J. Gosse, G. F. Hewitt,
M. Majcen, T. Mizushina, V. K. M. Sastri,
S. Sideman, H. C. Simpson,
M. A. Styrikovich, and D. A. de Vries

Volume 2

GENERAL PAPERS

Conduction
Natural Convection
Environmental Heat Transfer
Radiation

Organized under the authority of
the Assembly for International Heat Transfer Conferences

in cooperation with
the International Scientific Committee
the Deutsche Gesellschaft für Chemie- und
Verfahrenstechnik (DGCV)
and the German Scientific and Executive Committees

by

DECHEMA
Deutsche Gesellschaft für chemisches Apparatewesen e.V.,
Frankfurt/Main, Fed. Rep. of Germany

HEMISPHERE PUBLISHING CORPORATION
Washington New York London